43

Reprinted from the Technology of Nuclear Magnetic Resonance


# OVERVIEW OF NMR RECONSTRUCTION PRINCIPLES

T.M. Peters and B.C. Sanctuary

Montreal Neurological Institute, Montreal, Quebec, Canada

## ABSTRACT

This paper describes two approaches to image reconstruction in nuclear magnetic resonance: projection reconstruction and two-dimensional Fourier ("spin-warp") imaging. Both these procedures are based on use of the field gradients as a means of spatially encoding the spins in an NMR imaging system. The physical principles of all procedures are examined in detail.

## INTRODUCTION

In classical NMR experiments, measurements are made on a sample located in a highly uniform magnetic field with a homogeneity of up to one part in one hundred million (1). The rf signal received by the system nevertheless consists of oscillations of more than a single frequency, and in general the spectrum will exhibit peaks separated by small frequency differences (parts per million). These multiple resonances are caused by the local magnetic shielding resulting from the interaction between electrons associated with the nuclei and the applied magnetic field. This shielding effect changes the local magnetic field, thereby raising or lowering the Larmor precession frequency. The rf signal recorded under these conditions is therefore characteristic of a particular chemical environment. Compounds that have nuclear spins have unique spectra, and these spectra can be used to analyse or characterise chemical samples. The relative displacement of peaks in the spectrum is known as chemical shift.

Classical NMR techniques were based on swept frequency excitation procedures (2), but with the advent of digital computers, and particularly the Fast Fourier Transform algorithm (3), Fourier transform spectroscopy developed rapidly (1). This technique enables all the frequencies radiated by the sample to

be measured at once, with the individual components being unscrambled by means of the Fourier transform.

NMR spectroscopy tells us nothing about the spatial distribution of the substance within the sample; instead, it suggests its chemical composition. To perform imaging on a sample we must trade off the ability to observe chemical shift for the ability to perform spatial localisation.

## FIELD GRADIENTS AND FOURIER TRANSFORMS

To use NMR for imaging, we must destroy the magnetic field homogeneity so desirable in spectroscopy by introducing a controlled spatial variation of the magnetic field, usually in the form of a linear "gradient" applied in one or more of the three orthogonal directions. A magnetic field gradient then enables us to vary the strength of the magnetic field with position. If we perform an experiment on a sample that has, for example, three components spaced at equal distances along a tube in the z direction, and if we impose a z-directed gradient on the main field, after exciting all of the nuclei into precession we obtain a composite rf signal consisting of three distinct frequency components. These locate the three regions of the sample (Fig. 1).

Fortunately, the Fourier transform of the received signal both quantifies each frequency and locates each component in the tube. The magnetic field gradient gives each "slice" of the tube a unique magnetic field and thus its own precession frequency. The process of resolving the recorded signal into its frequency components then produces a "map," a one-dimensional image, of the distribution of the sample in the z-direction. In NMR imaging the field gradient and the Fourier transform of the received signal are therefore essential for obtaining information about the spatial distribution of the sample.

This relationship between precession frequency and spatial location may be represented as follows:

| | |
|---|---|
| Main field strength (z direction) | $= B_0$ |
| Precessional frequency ($B_0$ only) | $= 2\pi\gamma B_0$ |
| Precessional frequency in presence of gradient $G_z$ | $= 2\pi\gamma(B_0 + zG_z)$ |

Under these conditions the signal generated by the precession of any NMR nucleus at position z is

$$s_z(t) = D(z)e^{j2\pi\gamma(B_0 + zG_z)t} \qquad (1)$$

where D(z) is related to the density of the nuclei at position z. For a particular value of $\gamma$ (the gyromagnetic ratio that relates the precession frequency to the magnetic field), equation (1) states that at each position z we have a precessional frequency f given by

$$\omega(z) = 2\pi\gamma(B_0 + zG_z) \tag{2}$$

This variable field in the z direction indicates that each component in the axial direction is experiencing a different magnetic field and will therefore resonate with a different frequency. The signal that we measure is therefore the integral of all the individual components along the length of the sample. Mathematically we express this signal as a function of time as follows:

$$s(t) = \int_{z_1}^{z_2} D(z)e^{j2\pi\gamma(B_0 + zG_z)t}dz$$

$$= e^{j2\pi\gamma B_0 t}\int_{z_1}^{z_2} D(z)e^{j2\pi\gamma zG_z t}dz \tag{3}$$

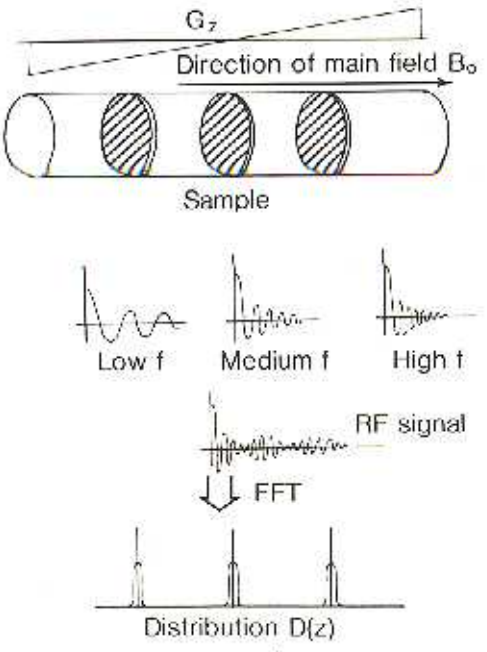


FIG. 1

Hypothetical NMR sample; $G_z$ gradient field with protons only in 3 distinct planes. The composite rf signal is Fourier transformed to give a map of the proton density D(z) as a function of position.

The first part of the right side of this expression is simply the Larmor frequency in the presence of the main field without a gradient. This sinusoidal oscillation is modulated by the integral of all of the signals generated by nuclei making up the distribution D(z) in the sample and lying in the magnetic field defined by the gradient $G_z$.

In one-dimensional imaging (not a very useful procedure), our objective would be to determine the distribution D(z). (In this discussion we are not concerned with relaxation times $T_1$ or $T_2$ but only with the distribution of the nuclei being studied.) In order to extract the quantity D(z) from the signal s(t), we must first eliminate the high frequency modulation. We are then left with the required signal

$$s_1(t) = \int_{z_1}^{z_2} D(z) e^{j2\pi\gamma z G_z t} dz \qquad (4)$$

Because the product $k_z = -\gamma G_z t$ has the dimensions of 1/distance (or spatial frequency), we may make the substitution and rewrite this expression as

$$s_1(k_z) = \int_{z_1}^{z_2} D(z) e^{-j2\pi z k_z} dz \qquad (5)$$

which is recognisable as a standard Fourier transform pair. If we compute the inverse Fourier transform of $s_1(t)$, we obtain the quantity D(z), i.e.,

$$D(z) = \int_{-\infty}^{\infty} s_1(k_z) e^{j2\pi z k_z} dk_z \qquad (6)$$

which is the z distribution of the resonant nuclei in our sample. (c.f. Fig. 1)

We now know how the sample is distributed along one axis, but *little about its distribution in a plane or volume. Nevertheless*, the discussion has highlighted two important concepts. We started out with a time signal, which we detected and Fourier transformed (Eq. 4). The Fourier transform of this time signal was a distribution D(z) (Eq. 6) in space. If we compute the inverse Fourier transform of a spatial distribution, we of course calculate its spatial frequency components. But this inverse transform result is precisely the time signal with which we started. This equivalence of the measured time signal and the spatial frequency of the object is formalized by the change of variables made above (Eq. 5). So from this observation we may state: "Measurement time is proportional to spatial frequency," and "Spatial position is proportional to temporal frequency."

To understand NMR imaging concepts it is particularly important not to confuse the temporal frequency of the measured signal with the spatial frequency of the object distribution.

A second important concept derived from the preceding

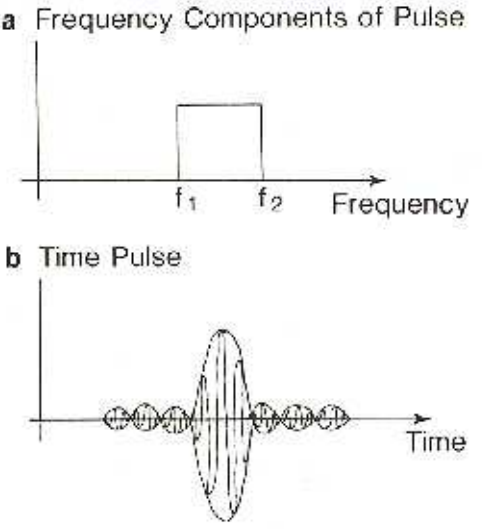


FIG. 2

Slice selection. In order to generate a signal whose frequency components occupy the required band (i.e., between $f_1$ and $f_2$) (a): we must transmit a time signal as shown by (b).

discussion is that we now see how we may isolate a single slice within an object. In the presence of a z gradient only, all nuclei in any transverse slice precess with a unique Larmor frequency. We can then excite a group of nuclei lying within a given plane by including in our rf excitation pulse only the frequencies pertaining to that plane (Fig. 2). Thus an initial rf pulse may be tailored to excite only nuclei in a selected slice.

## THE TWO-DIMENSIONAL FOURIER TRANSFORM

An image $i(x,y)$ has a Fourier transform $I(k_x,k_y)$ defined by the following expression:

$$I(k_x,k_y) = \int_{-\infty}^{\infty}\int i(x,y)e^{-j2\pi(k_x x + k_y y)}dxdy \qquad (7)$$

where $k_x$ and $k_y$ are spatial frequency coordinates (in units of inverse distance). The inverse Fourier transform is defined as

$$i(x,y) = \int_{-\infty}^{\infty}\int I(k_x,k_y)e^{j2\pi(k_x x + k_y y)}dk_x dk_y \qquad (8)$$

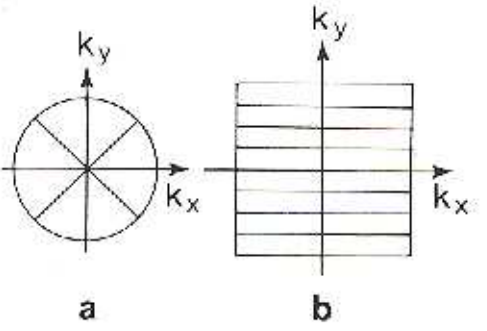


FIG. 3

k-(Fourier) space filling with back-projection reconstruction technique (a), and 2-D Fourier Zeugmatography technique (b).

In general the direct measurements of our NMR signal made in the presence of an imaging gradient will give us values in "k-space" or the $k_x,k_y$ spatial frequency plane. After determining $I(k_x,k_y)$ for a sufficient number of values of $k_x$ and $k_y$ we use a computer program to evaluate its inverse Fourier transform to determine $i(x,y)$. There are many imaging strategies for determining values of I for various $k_x,k_y$ (4,5). In this paper, we examine two of the most widely used, namely projection reconstruction (6) and Fourier zeugmatography (or spin-warp imaging) (7,8). The former is analogous to the means used by commercial CT scanners to reconstruct images from x-ray projections: filling of k-space in a spoke-like manner (Fig. 3a). The latter technique takes full advantage of the ability of the NMR imaging system to "explore" k-space in a raster fashion (Fig. 3b).

## PROJECTION RECONSTRUCTION

In figure 4, the disc is a slice selected perpendicular to the z direction (i.e., in the x-y plane). If we superimpose an "x" gradient on the main field such that its strength as a function of x becomes

$$B(x) = B_0 + xG_x \tag{9}$$

the precession frequency as a function of x is

$$\omega(x) = \omega_0 + x\gamma G_x \tag{10}$$

This implies that nuclei lying in y-directed strips a distance x from the origin are all precessing with the same frequency. The free induction decay signal, or "echo" (9), which will be recorded

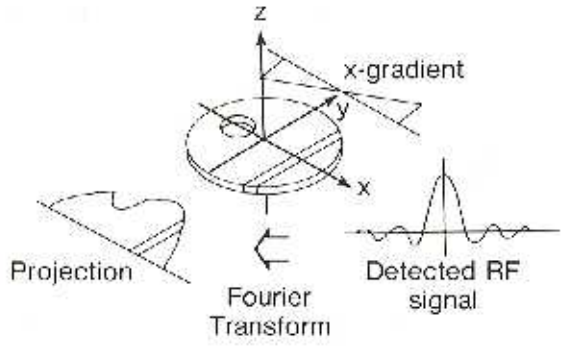


FIG. 4

Projection of a selected slice made in the presence of an x gradient.

following the slice selection rf pulse, will contain components from a band of frequencies defined by the Larmor precession rates corresponding to the range of magnetic field strengths within the extent of the object. Since all components within each strip precess with the same frequency, the signal, after Fourier transformation, will be a "y" directed projection of the precessing nuclei distribution within the slice (Fig. 4).

The central slice theorem (10), well known in CT, states that the Fourier transform of an object's projection made at an angle is equal to the values of the two-dimensional Fourier transform of the object along a line through the origin at the same angle. For the simple case of $\theta=0$, this is equivalent to determining the Fourier transform of the object along the $k_x$ axis in k space, i.e.:

$$I(k_x,0) = \int_{-\infty}^{\infty} \left[ \int_{-\infty}^{\infty} i(x,y) e^{-j2\pi k_y y} dy \right] e^{-j2\pi x k_x} dx \Big|_{k_y=0} \qquad (11)$$

The part of equation (11) in square brackets is the projection of i(x,y) parallel to the y axis. The remaining part yields the Fourier transform of this expression.

K-space can obviously be filled by taking successive projections at different angles, simply by using a combination of x and y gradients. Since magnetic fields add vectorally, a resultant "r" directed gradient may be easily synthesised. For each "r" gradient we determine "k" values along one radial line of the spokes in Fig. 3a. Although this approach was considered by many authors in CT reconstruction, problems with Fourier space interpolation and the errors generated thereby led to the evolution of the rho-filtered back-projection algorithm (11,12). While this formulation is mathematically equivalent, it is computationally more stable than techniques that perform explicit Fourier space interpolation.

In CT the measured projections are processed with a digital

filter whose frequency characteristic, at least at low frequencies, is proportional to $|\rho|$ where $\rho$ is the spatial frequency coordinate.

After filtering the projections in this manner, the data are back-projected onto a two-dimensional array at the angles $\phi$ from which the original measurement was taken. After all projections from all directions have been treated in this way, the array contains the reconstructed image (Fig. 5).

The procedure for reconstructing an NMR image from projections is very similar except that instead of the raw data being the projection of the object cross section, the measured NMR signal is already the Fourier transform of the projection. The appropriate "ρ-filter" may therefore be applied to the data directly, with the inverse Fourier transform yielding the properly filtered projection before the back-projection operation. Since this technique operates successfully in CT, one might assume it would also suffice for NMR reconstruction. However, it is well known in CT that the projection reconstruction technique over samples Fourier space towards the origin, with the result that the number of individual measurements required exceeds the number of resolution elements in the image by a factor of $\pi/2$ (12). Images recorded in this manner are also prone to exhibit streak artifacts if the patient moves during the scan, a particular problem with the longer scanning times in NMR.

An alternative and now widely used technique that employs the data more efficiently and is less prone to motion artifact generation is the two-dimensional Fourier reconstruction technique described below.

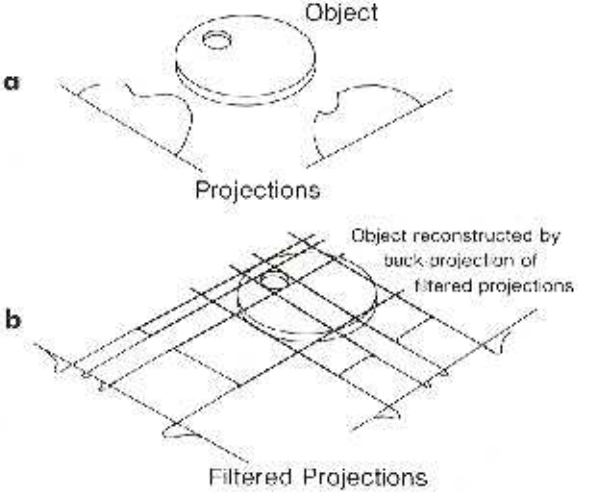


FIG. 5

a) Projections of an object;
b) Reconstruction by filtered back-projection.

## TWO-DIMENSIONAL FOURIER RECONSTRUCTION

Equation 6 may also be expressed as:

$$I(k_x;k_y) = \int_{-\infty}^{\infty}\left[\int_{-\infty}^{\infty} i(x,y)e^{-j2\pi k_y y}dy\right] e^{-j2\pi x k_x}dx \qquad (12)$$

Written like this, the Fourier transform of the image $I(k_x,k_y)$ may be interpreted as a series of projections of the object all parallel to the "y" axis but with the object pre-multiplied by a phase factor $e^{-j2\pi yk_y}$ before each projection measurement. When $k_y$=o we have the signal

$$I(k_x,0) = \int_{-\infty}^{\infty}\int_{-\infty}^{\infty} i(x,y)dy\ e^{-j2\pi x k_x}dx \qquad (13)$$

which is precisely the first measurement we made with the projection-reconstruction technique. From this point, however, the two procedures differ. Rather than generating a rotated gradient as for projection reconstruction, we manipulate the gradients to provide the phase factor pre-multiplication.

The nuclei along a particular "y" directed strip are each precessing at the Larmor frequency. If their relative phase is zero, they are precessing "in phase" with each other in such a manner that the total rf signal level they emit is a maximum (Fig. 6a). Applying a linear phase shift to all the spins in the "y"

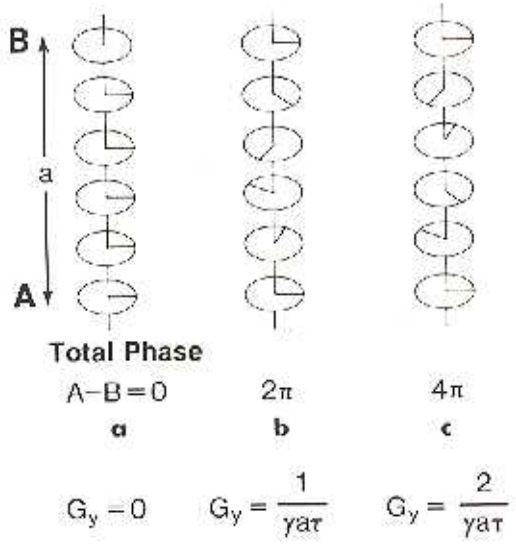


FIG. 6

Phase shifts with different strength encoding gradients, giving different total phase shifts between a and b.

direction implies that we progressively advance the relative phases of all the spins as we move up in y (Fig. 6b,c).

To illustrate, assume that the extent of the object i(x,y) in the y-direction is "a". To achieve a total phase delay of $2\pi$ radians across the object we would then need to set $k_y=1/a$ so that the "phase encoded" or "spin-warped" object of which we make a projection measurement is

$$i(x,y)e^{-j2\pi y/a}.$$

The signal recorded in the presence of an x-directed measurement gradient is no longer $I(k_x,o)$ but $I(k_x,1/a)$. In terms of the Fourier transform plane we have determined data along not the $k_x$ axis, but along a line parallel to it at a $k_y$ value of $k_y=1/a$. To determine N lines in k-space we may choose successive values of $\pm k_y$ in multiples of 1/a to achieve adequate sampling.

Unlike CT scanning, where we cannot phase encode the electron densities and hence must continue to use projection reconstruction, in NMR imaging we may perform this operation by manipulating the gradients. The the x-gradient is switched on during the read-out phase, thereby enabling spatial coding in the x-direction. To phase encode in the y-direction, we need only enable the y gradient for a short time.

The precession frequency in the presence of the main field and the y gradient is given by

$$\omega = \frac{d\phi}{dt} = 2\pi\gamma(B_o + yG_y) \tag{14}$$

where $\phi$ is the relative phase of the precession. Therefore the total phase accumulation after the application of the gradient field for a time $\tau$ is

$$\phi_\tau = 2\pi\gamma(B_o + yG_y)\tau. \tag{15}$$

The incremental phase change in the presence of the main field before and after the application of the encoding y gradient is therefore

$$\Delta\varphi_\tau = 2\pi\gamma yG_y\tau. \tag{16}$$

By selecting the strength of the y gradient field, and/or the time for which it is applied, we may impose any desired linear phase encoding onto the spin system. For a short time while the y gradient is applied, the spins speed up progressively along the y axis. As soon as the encoding gradient is removed, the nuclei return to their previous precession frequency, but with a controlled phase relative to each other. Each measurement with a different $G_y$ yields another line in k-space (Fig. 7), and we may continue in this manner until the Fourier transform of the image is adequately sampled. After filling up k-space to the desired resolution, all that is necessary to compute the image is a two-

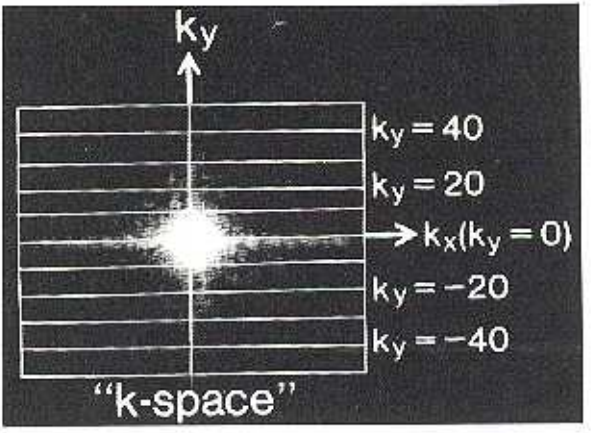


FIG. 7

k-space. The two-dimensional Fourier transform of an object, with the lines of k-space which are determined by application of several values of the phase encoding y gradient.

dimensional, inverse Fourier transform on the k-space array. In most commercial NMR units this procedure can be performed on a 256 x 256 point image using the fast Fourier transform algorithm in a matter of seconds.

## CONCLUSION

To simplify the explanation of these two approaches to image reconstruction in NMR, the effects of $T_1$ and $T_2$ relaxation times, digitising problems, and aliasing effects have deliberately been ignored in order to focus on the image reconstruction procedures themselves. The fundamental tools in NMR imaging are the magnetic field gradients and the ability to manipulate them and the fast Fourier transform algorithm, which can rapidly and efficiently calculate the spectra of one- and two-dimensional signals.

## ACKNOWLEDGMENTS

In preparing this paper we wish to acknowledge the many fruitful discussions with our colleagues, particularly Dr. R. Ethier. We wish to thank M. Longtin and G. Limoges for preparing the manuscript and the MNI Medical Photography Unit for preparing the illustrations.

## REFERENCES

1. Shaw D: Fourier Transform NMR Spectroscopy. New York, Elsevier, 1976.

2. Jackman LM: Applications of Nuclear Magnetic Resonance Spectroscopy In Organic Chemistry. New York, Pergamon,1959
3. Cooley JW and Tukey JW: An algorithm for the machine calculation of complex Fourier series. Math Commut 19:297-301, 1965
4. Twieg DB: The k-trajectory formulation of the NMR imaging process with applications in analysis and synthesis of imaging methods. Medical Physics 10 (5): 610-621, 1983
5. King K and Moran PR: A unified description of NMR imaging, data collection and reconstruction. Medical Physics (in press), 1984
6. Lautebur PC and Lai CM: Zeugmatography by reconstruction for projections. IEEE Trans Nucl Sci NS-27: 1227-1231, 1980
7. Edelstein WA, Hutchison JMS, Johnson G and Redpath I: Spin - warp NMR imaging and applications to human whole body imaging. Phys Med Biol 25(4): 751-756, 1980
8. Kumar A, Welti D and Ernst RR: NMR-Fourier zeugmatography. J Magn Reson 18: 69-83, 1975
9. Mansfield P and Morris PG: Advances in Magnetic Resonance Suppl. 2, NMR Imaging in Biomedicine Waugh JS ed. Academic Press, New York 1982, pp 46, 48
10. Barrett HH and Swindell W: Radiological Imaging 2, New York, Academic Press, 1981, pp 384-385
11. Lewitt RM: Reconstruction algorithms: Transform methods. Proc. IEEE 71:390-408, 1983
12. Smith PR, Peters TM and Bates RHT: Image reconstruction from finite numbers of projections. J Phys A: Math Nucl Gen 6:361-382, 1973